IEEE Access
Multidisciplinary | Rapid Review | Open Access Journal

Received November 5, 2021, accepted December 9, 2021, date of publication December 14, 2021,
date of current version December 28, 2021.

Digital Object Identifier 10.1109/ACCESS.2021.3135698

Tumor Depth and Size Perception Using a Pneumatic Tactile Display in Laparoscopic Surgery

HOANG HIEP LY[1,2], YOSHIHIRO TANAKA[1], (Member, IEEE), AND MICHITAKA FUJIWARA[3]

[1]Department of Electrical and Mechanical Engineering, Graduate School of Engineering, Nagoya Institute of Technology, Nagoya 466-8555, Japan
[2]Japan Society for the Promotion of Science, Tokyo 102-0083, Japan
[3]Medical xR Center, Nagoya University Graduate School of Medicine, Nagoya 466-8550, Japan

Corresponding author: Hoang Hiep Ly (h.ly.944@nitech.jp)

This work was supported in part by the Japan Society for the Promotion of Science (JSPS) under Grant-in-Aid (KAKENHI) for JSPS Fellows (Grant number: JP19J23169) and for Scientific Research (Grant number: JP17H01252).

ABSTRACT Tumor location, depth, and size are essential information for tumor resection surgery. In open surgery, surgeons can obtain information by palpating the tissue with their fingers. In minimally invasive surgery, where the natural sense of touch is restricted, surgeons can rely on haptic information provided by haptic devices to determine the tumor characteristics. Tactile feedback is a promising representation modality for providing haptic information intuitively to surgeons during tissue palpation. In this paper, we propose a palpation strategy using tactile feedback to determine the tumor depth and size. For the palpation strategy, the tumor depth was determined by detecting the presence of the tumor at a given indentation depth of the sensor. Tumor size may be obtained by localizing the tumor edges. Fundamental experiments were conducted to investigate the use of contact force components in determining tumor features using the proposed strategy. The results indicated that the normal force is more useful in estimating the indentation depth, and the shear force is highly effective in detecting tumor regions and edges. Users' ability to characterize the tumor using tactile feedback from our developed tactile display was demonstrated through tissue palpation tasks. Participants who received both normal force and shear force feedback could identify the depth and size of the embedded tumor with 66 % and 65 % accuracy, respectively. These results suggest that tactile displays that provide normal and shear force feedback can be successfully used for tumor characterization.

INDEX TERMS Minimally invasive surgery, pneumatic tactile display, tumor characterization, tactile feedback.

I. INTRODUCTION

Over the last few decades, minimally invasive surgery (MIS) has become a common surgical procedure. MIS offers many medical advantages over traditional open surgery, such as less postoperative pain, shorter recovery time, and better cosmetic healing. However, this surgery has some limitations. Surgeons have to cope with constrained motion and limited visual information of the tissue during surgery. In addition, MIS eliminates the natural haptic sensation, resulting in the risk of tissue trauma during surgery [1], [2]. Haptic information in MIS might enable surgeons to perform safer operations.

In tumor resection surgery, characteristics such as the location, depth, and size of the tumor are important information. If surgeons know the characteristic information, they can resect the entire tumor with a minimum margin without interfering with the function of surrounding tissue or remaining organs [3], [4]. Generally, advanced imaging techniques such as magnetic resonance imaging (MRI) and computed tomography (CT) can be used to characterize tumors preoperatively [5]. These techniques can provide an accurate image of the location of the tumor and its mechanical properties such as depth, size, and chemical structure [6]. These preoperative imaging approaches are effective for rigid structures, such as skulls or bones, but are challenging for soft tissue. Shifting intraoperative organs and soft tissue deformation during a surgical procedure can complicate the accurate registration of a tumor, and preoperative information is not completely

The associate editor coordinating the review of this manuscript and approving it for publication was György Eigner.

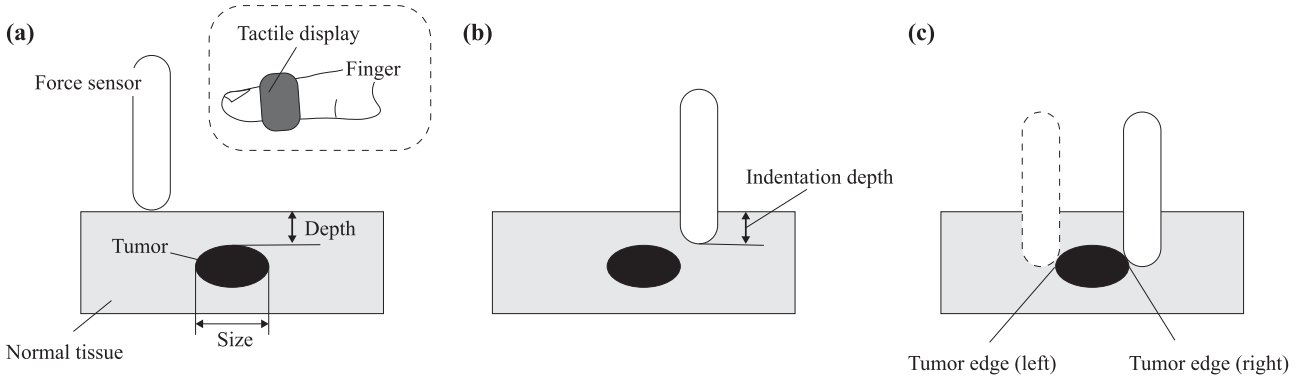

FIGURE 1. Illustration of the proposed tissue palpation strategy. (a) Tissue model with embedded tumor and haptic devices for the tissue palpation. (b) Tumor depth determination. (c) Tumor size determination.

reliable [5], [7]. A promising approach to obtaining tumor characteristics is the use of palpation techniques during the surgery. In open surgery, surgeons can rely on the tactile sensation of their fingers to palpate and explore the tumor [8], [9]. In MIS, which has no direct tactile sensation, the haptic sensation from haptic devices can be used to examine abnormal tissue [10].

Haptic information can be provided to surgeons using various methods. Talasaz and Patel [11] and Gwilliam *et al.* [10] used tactile array sensors to construct force distribution images when palpating target tissue. Yamamoto *et al.* [12] and Liu *et al.* [13] collected discrete and continuous force data using single–point force sensors to obtain the graphical stiffness mapping of the soft tissue examined. The location and size of the embedded tumor were reflected in tactile images. The movements of these sensors in tissue palpation were driven by a robotic or automated stimulation system. The tumor depth was obtained using the indentation displacements of the force/tactile sensors. Although visual feedback methods can provide relatively useful information on the mechanical tissue properties, the results of tumor characterization are often affected by several factors during data collection. For example, if high contact stresses occur at the edges of the sensor array or the indentation depth of the force sensor is not maintained at a constant level during palpation, the constructed force image may be degraded. Additionally, the use of visual feedback to interpret the tissue information might overload the visual channel for surgeons because they have to focus on laparoscopic imaging during surgery [14]. Instead of graphical representation, recent research has focused on analyzing force data using haptic perception algorithms to obtain tissue characteristics. Computational models established using artificial neural networks [7], [15] and deep current neural networks [16] have been used to identify the size and depth of abnormal tissue. Other researchers have proposed models for estimating the characteristics of tumors using a finite–element–based method [17] or a dynamic position sensing method [18]. These computational models can determine the size and depth of the tumor with high accuracy. However, the performance of these methods is highly dependent on the data collected, complicating their application to various tissue. Furthermore, the sensors for collecting the data must be moved by an automated system, such as a robot. Thus, the proposed methods can only be applied to robot–assisted MIS.

Tactile feedback is a promising alternative for providing haptic information to surgeons during intraoperative tissue palpation. Tactile feedback not only provides an intuitive understanding of tissue properties, but it is also independent of the visual channel; thus, it rarely impedes the surgeon's operation. Numerous actuation methods have been employed to generate the tactile feedback for tissue palpation, such as tactile displays using shape memory alloy wires [19], multiple servomotors [20], and pneumatic systems [21] to drive pin-array elements to represent the spatially distributed reaction force. Bianchi *et al.* [22] and Rizzo *et al.* [23] utilized pneumatic air–jet and magnetorheological–fluid (MRF) devices, respectively, to display lumps (or tumors) of different sizes. Although these tactile displays can provide information about tumor shape, size, or stiffness, the perception of tumor depth is arguable. In addition, these devices are often large and complex. They are expensive to manufacture because they consist of multiple display elements, large drive units, and tactile array sensors to acquire tactile information. Thus, the tactile display may not be used as a disposable device for widespread surgical applications.

Fukuda *et al.* developed a tactile ring that uses pneumatic power to provide instantaneous tactile feedback to assist surgeons in tumor localization [24]. This tactile display has high clinical applicability owing to its simple structure, low cost, disposability, and robustness to sterilization. Utilizing this type of tactile display, we proposed a ring–type tactile display (SuP–Ring) with two force–feedback functions for tissue palpation [25]. The tactile display employs normal indentation, a substitutional modality, driven by pneumatic power to produce normal and shear force feedback. In the tactile display, the shear feedback is provided independently of normal feedback regardless of the friction between the tactile elements and human skin as the other tactile display uses lateral skin stretch, a popular feedback modality, in which

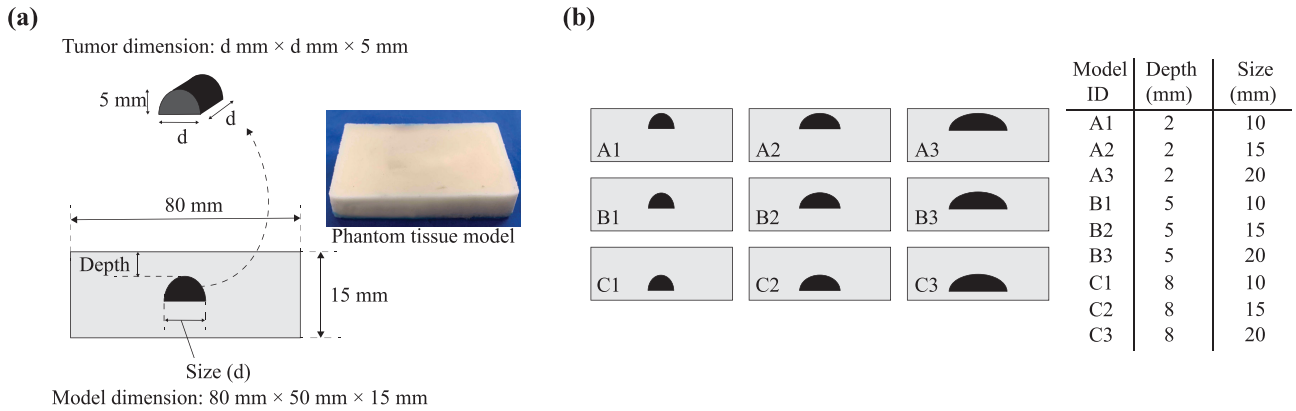

Model ID	Depth (mm)	Size (mm)
A1	2	10
A2	2	15
A3	2	20
B1	5	10
B2	5	15
B3	5	20
C1	8	10
C2	8	15
C3	8	20

FIGURE 2. Artificial phantom tissue model. (a) Structure of the tissue model. (b) The dimension of tissue models and the embedded tumors.

a shear force is applied to the skin. Moreover, the shear force feedback of the display can improve the performance of locating tumors, and the normal feedback can contribute to maintaining the safety requirements of MIS. Although the tactile devices described above have been effective in localizing tumors intraoperatively, their ability to characterize tumors has not been considered. Konstantinova *et al.* reported that the use of a combination of normal (related to normal force) and lateral (related to shear force) motions is more effective in exploring hard nodules (or tumors) [26]. Thus, we assumed that the provision of both normal and shear force feedback, such as SuP–Ring, might be effective in assessing characteristics such as tumor depth and size.

We propose a palpation strategy with a force sensor and a tactile display to identify the depth and size of the abnormal tissue (Fig. 1). The user palpates the tissue using the force sensor, and the force feedback of the tactile display provides the user with contact force information. First, the user estimates the indentation depth of the force sensor based on the provided force feedback (Fig. 1(b)). Subsequently, they attempt to determine the tumor's depth by detecting its presence at the indentation depth of the given sensor. Furthermore, we assume that the size of the tumor can be obtained by localizing the tumor edges using force feedback. As shown in Fig. 1(c), if the left and right edges of the tumor are located, the entire tumor area (or the tumor size) can be determined.

In this study, we aimed to assess the use of normal and shear feedback to identify tumor depth and size during laparoscopic tissue palpation. First, fundamental experiments were conducted to investigate the response of the contact force components during tissue examination. Several artificial phantom tissue models with embedded tumors of different sizes and depths were prepared for the experiment. The experimental results revealed which contact force components are effective in determining the tumor depth and which components are useful in determining the size of tumors based on the proposed palpation strategy. Next, we conducted psychophysical experiments to investigate the user's ability to determine the tumor's depth and size using tactile feedback from a tactile display. Participants with no medical background were requested to wear our developed tactile display and perform palpation tasks with artificial phantom tissue models. They were required to respond to the depth and size of the embedded tumor within the examined tissue under three feedback conditions (of the tactile display): only normal force feedback, only shear force feedback, and both normal and shear force feedback. The experimental outcomes were used to evaluate the identification performance.

II. MATERIALS AND METHODS

A. FUNDAMENTAL EXPERIMENTS

Fundamental experiments were designed to assess the response of contact force components, including normal and shear forces, for tumor characterization. In the experiments, we established an automated tissue palpation setup that provides accurate and consistent force responses for evaluation.

1) PHANTOM TISSUE MODELS WITH EMBEDDED TUMOR

Nine artificial phantom tissue models with embedded tumors were prepared. The dimensions of each model were 80 mm × 50 mm × 15 mm (Fig. 2). The tissue models were fabricated from pourable urethane rubber (Young's modulus: 6 kPa) using a 3–D printed mold. Semi–cylindrical tumors with a height of 5 mm, a square base, and side lengths (d) of 10, 15, and 20 mm (as the size of the tumor) were fabricated from silicone rubber (Young's modulus: 28 kPa), as shown in Fig. 2(a). The tumors were embedded at depths of 2, 5, and 8 mm from the surface of the tissue models. The depth and size of the embedded tumor in the models were within the depth range (0–30 mm) [4] and size range (6–160 mm) [3] of hepatocellular carcinoma. The identity (ID) of the phantom tissue model and the location, size, and depth of each embedded tumor are shown in Fig. 2(b). The stiffness of normal (phantom) tissue is similar to that of the human liver (ranging from 4 to 6.5 kPa) [27]. In comparison, the embedded tumor stiffness matched the hepatocellular carcinoma range (20.4–75 kPa) [28].

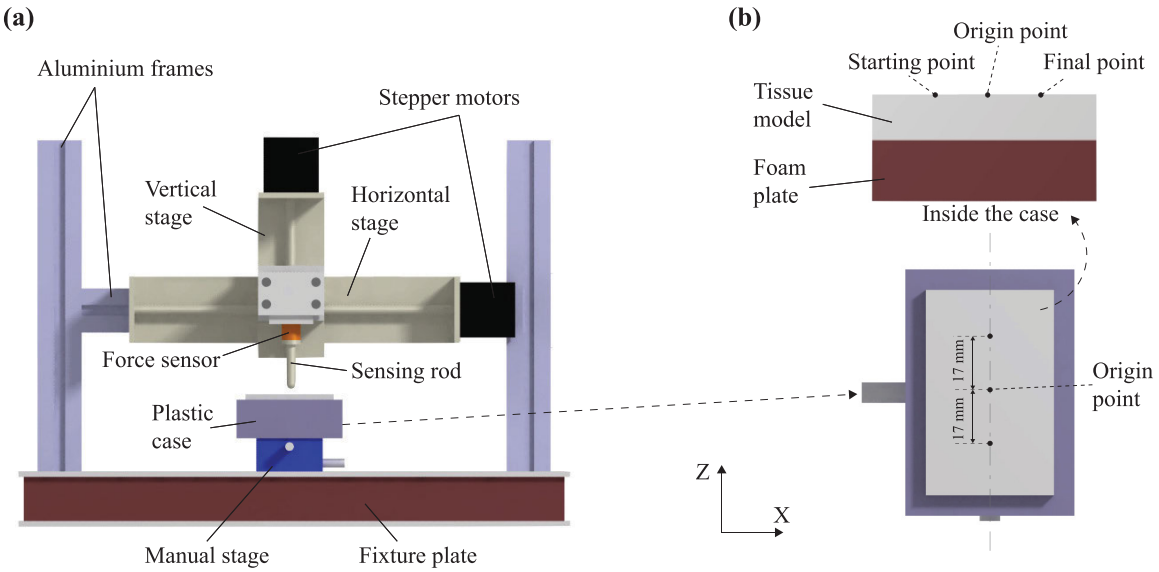

FIGURE 3. Setup of the fundamental experiment. (a) Front view of the setup. (b) Tissue model setup.

2) EXPERIMENTAL SETUP

Fig. 3(a) shows the experimental setup using the prepared tissue models. A 6–axis force/torque (F/T) sensor (Nano 17, ATI, Inc.) was employed to measure the contact force. A sensing rod with a hemispherical tip (diameter of 8 mm), fabricated from photopolymer resin (clear resin 1 L) using a 3–D printer (Form 3, Formlabs, Inc.), was attached to the sensor. The rod was used as a sensing component that directly contacted the tissue models. The force sensor was mounted on an adjustable stage (vertical stage), which was fixed on another adjustable stage (horizontal stage). The horizontal stage was mounted on a stand established from the aluminum frames. Stepper motors adjusted the movement of the stages. The phantom tissue model was placed on a polyurethane foam plate with dimensions of 80 mm × 50 mm × 20 mm (Fig. 3(b)). The foam plate simulated the soft tissue (or organ) beneath the evaluated human tissue (liver tissue). The phantom tissue model and foam plate were placed in a plastic case to hold them in position. The case was fixed on a 2–axis manual stage to adjust the position of the phantom tissue model.

3) EXPERIMENTAL PROCEDURES

Some essential points were defined in the fundamental experiment. The central point on the surface of the phantom tissue model was defined as the origin point, with $Z = 0$ mm and $X = 0$ mm (Fig. 3(b)). The initial point was 5 mm above the origin. The starting point was a point on the surface of the phantom tissue model, which was 17 mm to the left of the origin (with $Z = 0$ mm and $X = -17$ mm). The final point (with $Z = 0$ mm and $X = 17$ mm) was symmetric to the starting point through the origin (Fig. 3(b)). The tip of the sensing component (the sensing tip) was adjusted using the vertical and horizontal stages. The collection cycle was conducted as follows:

First, the vertical stage was adjusted to move the sensing tip along the z–axis away from the tissue surface ($Z = 0$ mm). At the surface of the model, the normal and shear force outputs of the sensor were set to 0 N to eliminate the effect of the initial noise. The stage was moved from $Z = 0$ mm to $Z = 14$ mm in 2 mm increments to increase the applied force. At each increment (collection point), the tip was stopped for 1 s to collect the components of the contact force, including normal and shear forces (z–axis and x–axis forces, respectively). Subsequently, the sensing component was rapidly returned to the tissue surface ($Z = 0$ mm), and the collection cycle was completed.

In the experiment, the sensing tip moved from the initial point to the origin. At the origin, the applied force was zero. Next, the tip was moved to the starting point by adjusting the horizontal stage. A collection cycle was conducted at the starting point. Subsequently, the horizontal stage was used to adjust the position of the tip in the x–axis direction from the starting point to the final point in increments of 2 mm. A collection cycle was applied at each increment. After the data was collected at the final point, the tip was returned to the initial point. Experiments were conducted on the nine prepared models.

4) DATA ANALYSIS

a: DATA PREPARATION

In the fundamental experiments, we aimed to evaluate the effectiveness of the force component in identifying the depth and size of the embedded tumor. The raw normal and shear force outputs tended to have different ranges of values. Thus, the raw data were normalized to the range 0–100 to provide the two force components an equal scale [29].

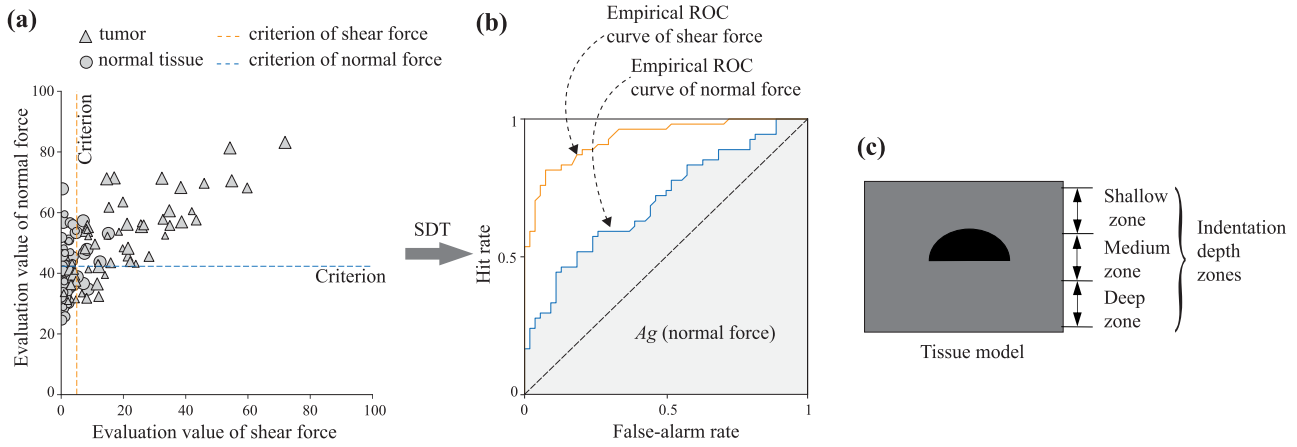

FIGURE 4. Detection sensitivity of contact force components for tumor detection by signal detection theory. (a) Tumor detection by criterion. (b) ROC curves of normal and shear force for tumor detection. (c) Indentation depth zones of the sensor.

The normalized values (called evaluation values, E) were calculated as follows:

$$\mathrm{E} = \frac{F - F_{\min}}{F_{\max} - F_{\min}} \times 100, \tag{1}$$

where F is the absolute value of the measured normal (or shear) force at each collection point in each tissue model. $F_{\min}$ and $F_{\max}$ are the minimum and maximum absolute values of the measured normal (or shear) force within all collection points from the nine tissue models, respectively. In this experiment, the $F_{\min}$ values were 0 N at the tissue surface for both measured force components.

b: DETECTION SENSITIVITY

According to the proposed palpation strategy for determining tumor features, the indentation depth of the sensor should first be estimated from the contact force information. The indentation depth of the sensor was divided into three depth zones: shallow (2–6 mm), medium (6–10 mm), and deep (10–14 mm) according to the depth of the tumor embedded in the nine tissue models (Fig. 4(c)). Assuming that the indentation depth zones were obtained, we had to locate the tumor in each depth zone to determine the tumor depth. Similarly, to determine the size of the tumor, we had to identify the edge of the tumor over the depth zones. Overall, to assess the ability of normal and shear forces to determine tumor features, we investigated the sensitivity of the force components in distinguishing between the tissue area with and without tumors. For example, when we obtained the contact force data for all tissue models in fundamental experiments, the Cartesian display of the evaluation values of the normal and shear forces in the deep zone could be shown in Fig. 4 (a). A simple method of detecting the tumor area is to select an appropriate criterion for each force component. Since the force response of the tissue area with tumor tends to be higher than that of the tissue area without the tumor, if the evaluation value of the force component is greater than the criterion, it is classified as ''tumor.'' Conversely, if the evaluation value is lower than the criterion, it is classified as a ''normal tissue'' (or ''no tumor'') (Fig. 4 (a)). This classification method is rooted in signal detection theory (SDT) [30]. The tests using this classification method can be evaluated using a hit rate $H \in [0, 1]$ (the ratio of ''tumor'' class response when a tumor is present) and a false alarm rate $F \in [0, 1]$ (the ratio of ''tumor'' class response when a tumor is absent). The values of hit and false alarm rates are based on the selected criterion, which is a scale from 0 to 100 (according to the range of the evaluation value). If the sensitivity of the force component is good, the hit rate approaches 1, and the false alarm rate approaches 0. However, there is no way to select a criterion that achieves only hits ($H = 1$) and no false alarms ($F = 0$) for all tissue models. With SDT, we can analyze the empirical receiver operating characteristic (ROC) curve of each force component response to remove the effect of the selected criteria. The ROC curve indicates pairs of (F, H) for the different criteria. To obtain the ROC curves for each normal and shear force response, the criteria vary from low to high levels (from 0 to 100 with an increment of 1). The area under the ROC curve can be used as a sensitivity index to assess the sensitivity of each force component information in detecting the tumor area (Fig. 4 (b)). The sensitivity index (A_g) was computed as follows [30]:

$$A_g = \frac{1}{2} \sum_{0}^{N-1} (H_{i+1} + H_i) \times (F_{i+1} - F_i), \tag{2}$$

where (H_i, F_i) is the pair of hit and false alarm rates, and N is the number of criteria. A_g ranges from 0 to 1, with a chance level of 0.5. If the A_g value is less than the chance level, it means that the evaluated force component cannot distinguish between the tissue area with and without the tumor. A higher A_g value indicates that the evaluated force component can be more effective for tumor detection.

B. PSYCHOPHYSICAL EXPERIMENT

We conducted psychophysical experiments to assess the ability of users to identify abnormal tissue features. The users provided tactile feedback using our developed tactile display

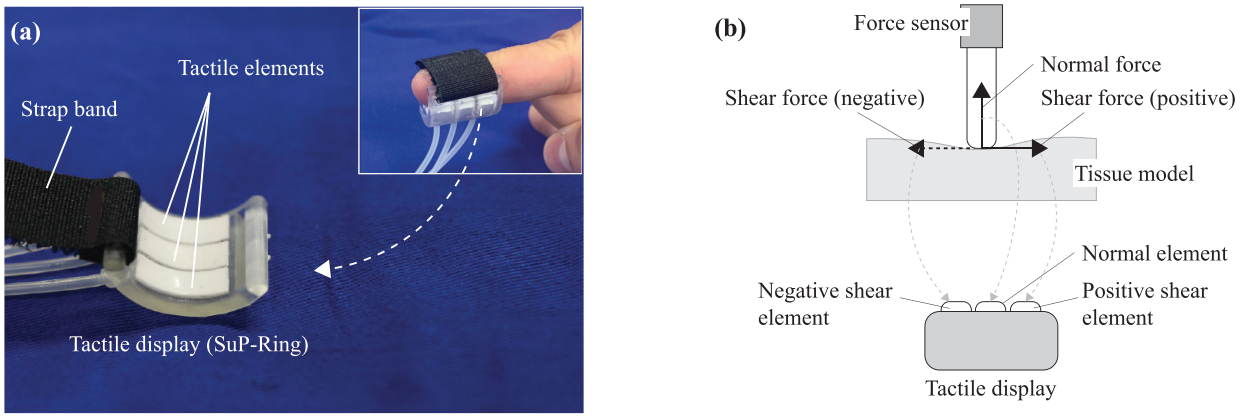

FIGURE 5. Tactile display. (a) Tactile display's prototype. (b) Operation mechanism of the tactile display.

and performed palpation tasks with artificial phantom tissue models. The effectiveness of the tactile feedback conditions in characterizing the tumor was analyzed using experimental results.

1) PARTICIPANTS

In this study, we aimed to examine the effects of tactile feedback on tissue palpation in a fair manner. Since skilled surgeons vary widely in their surgical skills and experience, novices were employed to reduce the influence of variation in the palpation experiments [24]. Ten participants, including seven men and three women (ranging in age from 23 to 28 years), without any medical background, participated in the experiments. All participants were right-handed according to the Coren test [31]. The participants consented to conduct the experiment with an experimental protocol according to the ethical standards of the Helsinki Declaration and approved by the Ethical Committee of the Nagoya Institute of Technology.

2) TACTILE DISPLAY

Fig. 5(a) shows the ring–shaped tactile display (SuP–Ring) using pneumatic power that we developed for laparoscopic tumor localization [25]. The tactile display consists of three tactile elements (silicone membranes): a normal element, a positive shear element, and a negative shear element. The normal indentations generated from these tactile elements provide tactile feedback to the users. This display method can represent the shear force independently of the normal force without being affected by the friction between the tactile elements and human skin, as in the other tactile display that employs other feedback representation methods such as the lateral skin stretch method. In addition, because the SuP–Ring is lightweight and has a ring shape, it can be easily worn on the user's fingers and rarely impedes the surgeon's movement during operation. Furthermore, this tactile device is sterilizable and disposable, making it highly clinically applicable.

The SuP–Ring provides the relative pressure based on the force information from a force sensor according to the following formulas:

$$P_{\mathrm{N}} = \begin{cases} P_{\mathrm{N0}} + G_{\mathrm{N}} \times F_{\mathrm{N}}, & \text{if } P_{\mathrm{N0}} + G_{\mathrm{N}} \times F_{\mathrm{N}} \\ & \leq P_{\mathrm{threshold}} \\ P_{\mathrm{threshold}}, & \text{otherwise} \end{cases} \tag{3}$$

$$P_{\mathrm{SP}} = \begin{cases} P_{\mathrm{S0}} + G_{\mathrm{S}} \times F_{\mathrm{S}}, & \text{if } F_{\mathrm{S}} > 0 \text{ and } P_{\mathrm{S0}} \\ & + G_{\mathrm{S}} \times F_{\mathrm{S}} < P_{\mathrm{threshold}} \\ P_{\mathrm{threshold}}, & \text{if } F_{\mathrm{S}} > 0 \text{ and } P_{\mathrm{S0}} \\ & + G_{\mathrm{S}} \times F_{\mathrm{S}} \geq P_{\mathrm{threshold}} \\ P_{\mathrm{S0}}, & \text{otherwise} \end{cases} \tag{4}$$

$$P_{\mathrm{SN}} = \begin{cases} P_{\mathrm{S0}} + G_{\mathrm{S}} \times (-F_{\mathrm{S}}), & \text{if } F_{\mathrm{S}} < 0 \text{ and } P_{\mathrm{S0}} \\ & + G_{\mathrm{S}} \times (-F_{\mathrm{S}}) < P_{\mathrm{threshold}} \\ P_{\mathrm{threshold}}, & \text{if } F_{\mathrm{S}} < 0 \text{ and } P_{\mathrm{S0}} \\ & + G_{\mathrm{S}} \times (-F_{\mathrm{S}}) \geq P_{\mathrm{threshold}} \\ P_{\mathrm{S0}}, & \text{otherwise} \end{cases} \tag{5}$$

where P_{N}, P_{SP}, and P_{SN} are the representing pressure values of the normal, positive shear, and negative shear elements, respectively. F_{N} and F_{S} are the measured normal and shear forces, respectively. A maximum pressure value of $P_{\mathrm{threshold}} = 101.89$ kPa for the device's tactile elements was set to prevent these silicone elements from being ruptured. $P_{\mathrm{N0}} = P_{\mathrm{S0}} = 23.3$ kPa are the offset pressure values of the corresponding normal and shear force elements. $G_{\mathrm{N}} = 15.4$ kPa/N and $G_{\mathrm{S}} = 39.02$ kPa/N are the gain values of the normal and shear elements, respectively. The gain values were set such that the range of the air pressure for providing normal and shear feedback was the same, based on the results of the fundamental experiments. The bandwidth of the SuP–Ring is approximately 4.5 Hz [25]. Fig. 6 shows the relationships between the input force values and the corresponding (static) pressures represented at the three tactile elements of the SuP–Ring. The error bars indicated the standard deviations of 6 measurements. Generally, the normal

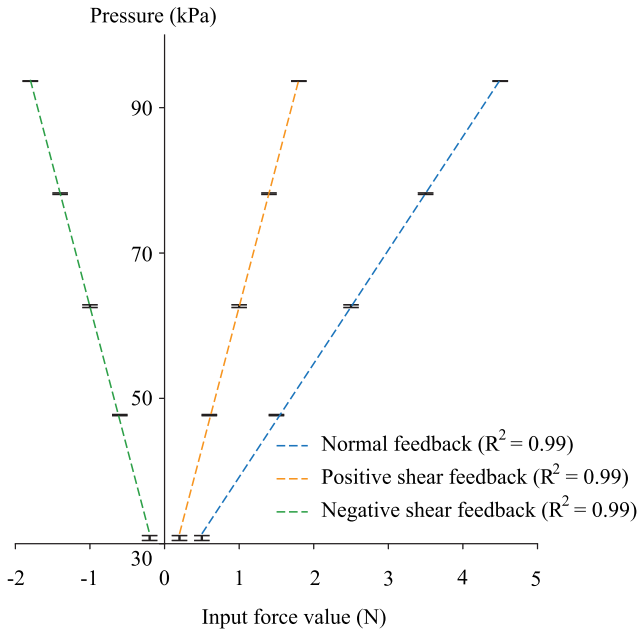

FIGURE 6. Static relationship between input force values and corresponding pressures (tactile feedback) represented at the three tactile elements of the tactile display.

and shear force feedback (pressures) provided by the tactile display are consistent. These feedback components are linearly related to the corresponding force inputs with the coefficient of determinations of 0.99 (for all tactile feedback). The feedback of shear force information from the tactile display enabled surgeons to detect the tumor within the normal tissue area, and the normal force feedback contributed to preserving the safety requirements for laparoscopic tumor localization, as reported in the previous study on the development of SuP–Ring [25].

3) EXPERIMENTAL SETUP

A tissue palpation experiment was designed to assess the user's ability to characterize the tumor using the SuP–Ring (Fig. 7). A similar experimental setup was used in our previous study to evaluate the effectiveness of the SuP–Ring in tumor localization. A palpated tool with a 6–axis F/T sensor (Nano 17, ATI, Inc.) and a sensing rod as the tool's sensing component, similar to the fundamental experimental setup, was used to measure the contact force. The tool can traverse vertically over a linear guide rail (A–rail), which can move horizontally over another linear guide rail (B–rail). The user can control the tool's tip position by moving the handle of the tool. The tactile feedback of the tactile display presented the normal force (z–axis force component) and shear force (x–axis force component) from the force sensor.

The phantom tissue model was the same as that used in the fundamental experiment. A ruler was attached to the case as a reference. Experimental images from the camera were displayed on a monitor mounted on the table. A wooden sheet simulating the abdominal wall was placed above the experimental setup with steel rods. Because of the wooden sheet, the user could obtain only visual information through the monitor.

4) EXPERIMENTAL PROCEDURES

The aim of the experiment was explained to the participants before conducting tissue palpation using the tactile display. Not all participants had experience with a tissue model with embedded tumors because they did not have a medical background. The participants need to know the tissue model they would be testing. Thus, we requested them to touch the tissue model with their index fingers to determine the depth and size of the embedded tumor. The operating mechanism of the tactile display was then demonstrated. The experiments were conducted under three conditions according to the feedback from the tactile display: normal feedback only (condition N), shear feedback only (condition S), and both normal and shear feedback (condition NS). In condition N, only normal feedback was provided to the users through the normal element of the tactile display. In condition S, the shear elements represent the shear force information, and the normal force information is ignored. In condition NS, three tactile elements of the tactile display were activated to provide both normal and shear force feedback to the user.

The participants wore the tactile display on their right-hand index finger pad and stood in front of the table to perform the tissue palpation experiment. The participants held the tool handle with their right hand. The participants palpated the phantom tissue models by moving the tool. The position of the tool's tip was observed via the monitor. The participants were informed that the embedded tumor was always located near the central point of the model. In the palpation experiment, the depth and size of the tumors were categorized into three types. For tumor depth, we defined "shallow," "medium," and "deep" depth corresponding to tumor depths of 2, 5, and 8 mm. For the size, "small," "medium," and "large" size were defined for tumors with sizes of 10, 15, and 20 mm. The participants were required to identify the tumor depth and size categories based on tactile feedback. They conducted training experiments to fully understand the experimental procedure before performing practical experiments to collect the necessary data. Each participant spent three days on the psychophysical experiments, including one day for the training experiments and two days for the practical experiments (Fig. 8(b)). Both training and practical experiments were conducted under three feedback conditions.

a: TRAINING EXPERIMENT

At the beginning of the training experiments, the participants examined the tissue model in the regions with and without tumors and felt the tactile feedback they received. They were requested to memorize tactile feedback in each region. After confirming that the participants could distinguish between the tumor and the normal tissue areas based on tactile feedback, they were requested to identify the tumor depth and size. For the tumor depth determination, the participants attempted to

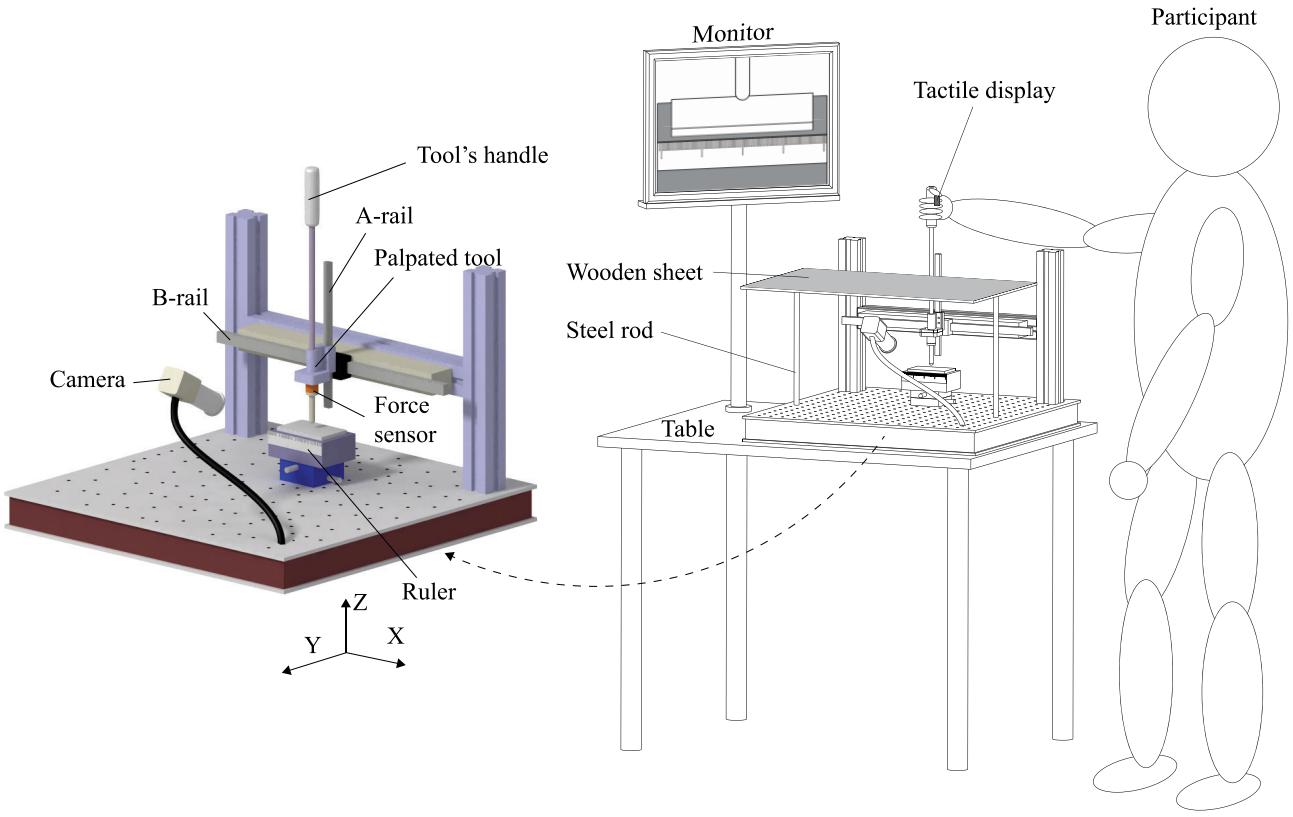

FIGURE 7. Laparoscopic tissue palpation setup.

detect the embedded tumor based on the tactile feedback provided. The participants were requested to examine the tissue model in all three indentation depth zones (shallow, medium, or deep). They determined the order of palpated depth zones. The depth zone was perceived based on the intensity of tactile feedback. The tumor depth (shallow, medium, or deep) was identified by determining the shallowest depth zone at which the participant detected the tumor. Regarding tumor size determination, the participants were requested to localize the edges of the tumor. Based on the location of the tumor edges and reference dimension with the ruler, the participants could identify the size of the tumors (small, medium, or large). During tissue palpation, since the depth and size of tumors often have a coupling effect on the force feedback [17], the edges of the (semi–cylinder) tumor may have been incorrectly detected when the participant palpated the tissue model in the inappropriate depth zone. For example, when a large tissue model with a medium depth tumor is palpated in the shallow depth zone, the participant might receive the same tactile feedback when a small tissue model with a shallow depth tumor is palpated in the shallow depth zone, resulting in incorrect detection of tumor size. Moreover, the results of fundamental experiments (to be mentioned in the next section) demonstrated that force feedback is capable of detecting all tumors in the deep depth zone only. Thus, the participants were instructed to examine the tissue model in the deep zones to accurately detect the location of the tumor edge. The training experiment consisted of two training sessions.

In the first training session, the depth and size of the embedded tumors were informed to the participants in advance. The participants palpated the tissue model to confirm the perception of tumor characteristics in each feedback condition. The main objective of the first training session was to aid the participants in identifying the tumor depth and size using tactile feedback from the tactile display. All tissue models were palpated under the three feedback conditions. There was no time limit for palpation during the training session. The participants were permitted to examine any tissue model repeatedly under any feedback condition until they were confident in identifying the tumor characteristics.

In the second training session, several phantom tissue models were randomly selected from the nine models. The participants were requested to determine the depth and size of the tumors embedded in the models. The aim of the training session was to practice palpating the tissue in a practical experimental scenario. One of the three feedback conditions was selected for the experiment. The tissue palpation task was performed within 60 s, and the participants were requested to complete the task as rapidly as possible. Completion time was recorded using a stopwatch. After 60 s, the participant had to immediately stop tissue palpation. After completing the task, the participants indicated their perceived depth

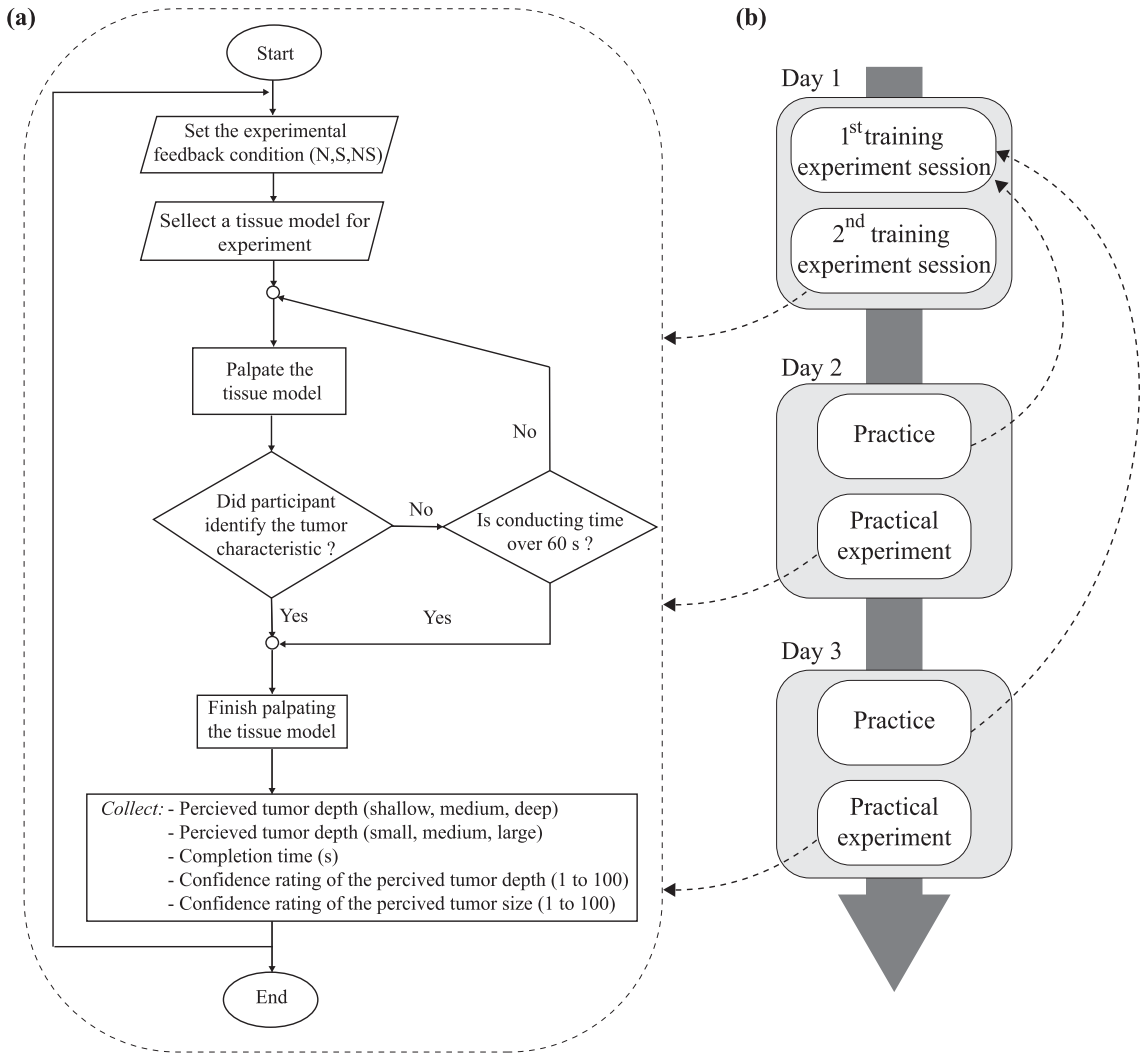

FIGURE 8. Experimental procedure. (a) Experimental procedure for each palpation task. (b) Experimental procedure for each participant.

(shallow, medium, or deep) and size (small, medium, or large) of the embedded tumor. They were also requested to provide the ''confidence rating'' for their identification of each tumor's characteristics. The ratings ranged from 1 (not confident at all) to 100 (very confident). At the end of each trial of the training session, the participants were informed of the actual information (the depth and size of the embedded tumor) of the model that they palpated. The participants could check the correctness of their identification. After completing the trial with the selected model, each participant took a break for approximately 30 s and then performed the tissue palpation task with other tissue models. The experimental procedure is shown in Fig. 8(a). In the second training session, each participant experimented with all feedback conditions in random order.

b: PRACTICAL EXPERIMENT

Before undertaking the practical experiment, the participants were permitted to practice palpating the tissue model several times in the same way as in the first training session. After they were confident about their perceptions, a practical experiment was started. In the practical experiment, all nine tissue models were examined one at a time for each feedback condition on each day. In each trial, the model was selected randomly. Each participant performed 54 trials over two days (27 trials each day), and ten participants conducted 540 trials in the practical experiments. The procedure of each tissue palpation trial in the practical experiments was the same as that in the second training session of the training experiments. After each trial, the participants responded to the identification of the tumor depth and size, as well as the confidence rating of each identification. In the practical experiment, we did not inform the participants of the correct characteristics of the implanted tumor at the end of each trial, as in the training experiment. During the experiment, participants were requested to wear headphones that produced white noise to eliminate the influence of other cues (such as sound noise from the pneumatic system) on the performance of

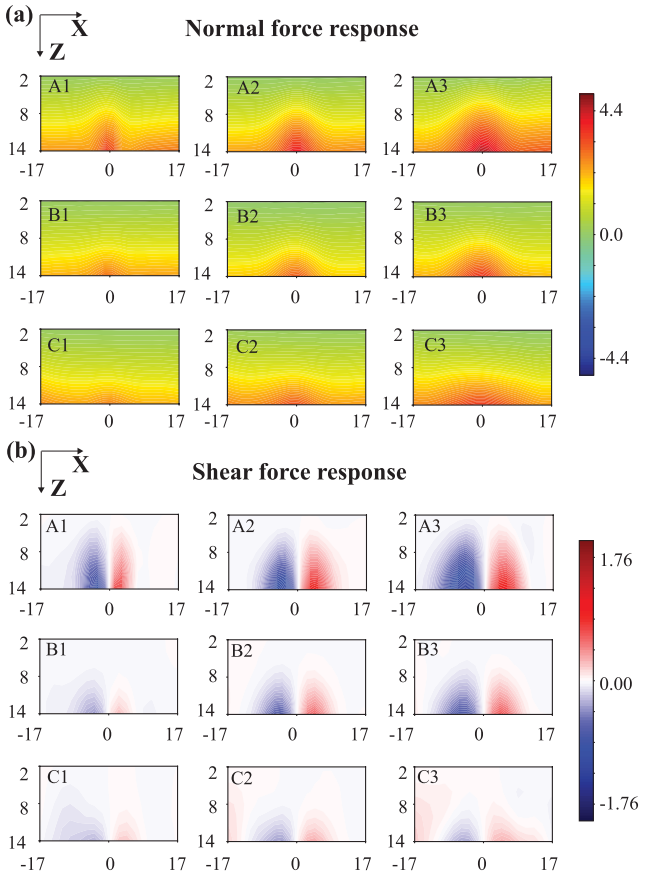

FIGURE 9. Results of the fundamental experiments. (a) Response of the normal force. (b) Response of the shear force.

the experiment. After completing tissue palpation in one condition, the participants took a 5–min break before moving to the next condition. Each participant spent approximately 1 h each day to complete the palpation tasks (27 trials) (about 2 h for two days). The participants conducted the experiment in different orders of feedback conditions on the two days of the experiment. The feedback condition order was also shuffled and partially counterbalanced across the participants.

III. RESULTS

A. FUNDAMENTAL EXPERIMENT

Fig. 9 shows qualitatively the contact forces measured from the force sensor of the nine tissue models in the experiment ($X \in$ [–17 mm, 17 mm] and $Z \in$ [2 mm, 14 mm]). The model IDs are shown in the corner of each image. Each image indicates the raw data of the normal force (Fig. 9(a)) or shear force (Fig. 9(b)) applied to each tissue model. The maximum absolute values of normal and shear force in the experiments were $F_{\max} = 4.64$ N and $F_{\max} = 1.53$ N, respectively. The obtained data were depicted and smoothed by contour plotting using Python.

1) INDENTATION DEPTH

Fig. 10 shows the relationship between the evaluation values of the normal (and shear force) and the indentation depth of

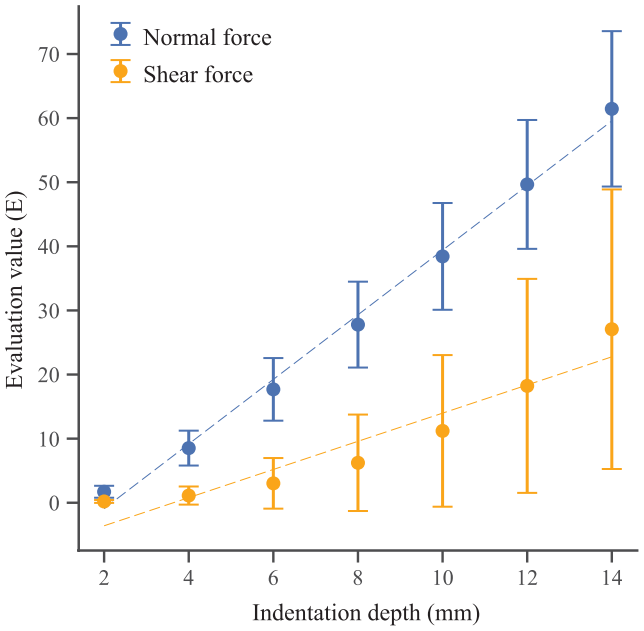

FIGURE 10. Relationships between the contact force components and the indentation depth of the force sensor.

the force sensor during the fundamental experiments. The evaluation values were computed from the raw data of all models according to Eq. (1). Pearson's correlation coefficient was used to evaluate the relationships. The results indicated a strong correlation between the evaluation value of the normal force and the indentation depth ($r(1134) = 0.94$, $p < 0.01$), and a moderate correlation between the evaluation values of shear force and indentation depth ($r(1134) = 0.46$, $p < 0.01$). This suggested that the use of normal force information is more effective in estimating the indentation depth of the sensor (or indentation depth zone).

2) TUMOR DEPTH DETERMINATION

From the above results, we can determine the indentation depth zone of the sensor using normal force information. Regarding the tumor depth determination, we need to investigate the sensitivity of the force component information for detecting the tumor area in each indentation depth zone.

The tissue model was divided horizontally (along the x–axis) into four evaluation regions: region 0 ($X \in$ [–17 mm, –11 mm]), region 1($X \in$ [–7 mm, –1 mm]), region 2 ($X \in$ [1 mm, 7 mm]), and region 3 ($X \in$ [11 mm, 17 mm]), as shown in Fig. 11(a). In all tissue models, the embedded tumors were located in regions 1 and 2 (the "tumor" region), while regions 0 and 3 were the normal tissue without the presence of tumor (the "no tumor" region). The means of the normal and shear force evaluation values in the "tumor" and "no tumor" regions were employed to assess the sensitivity of the force components for tumor detection.

Fig. 11(b) shows the sensitivity index of the two force components for three tumor depths in three indentation depth zones of the sensor, regardless of the tumor size. In the

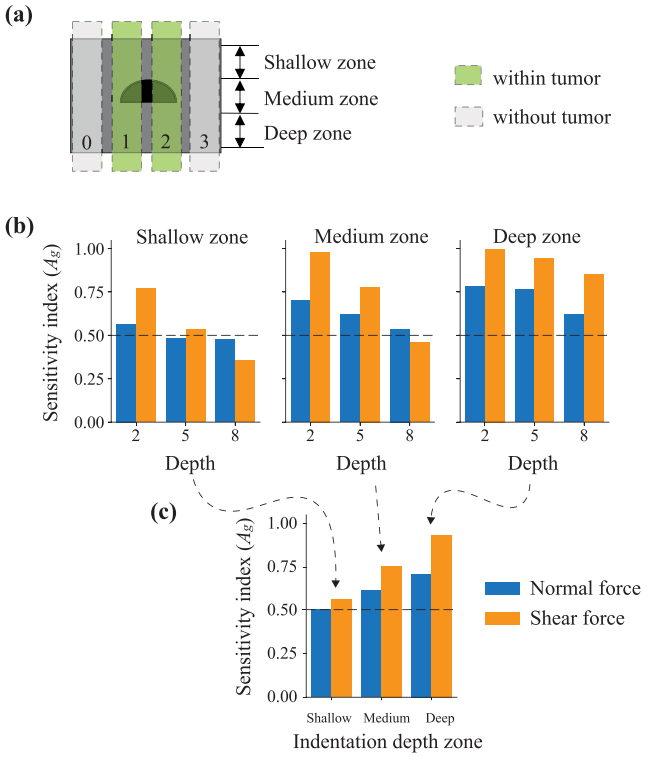

FIGURE 11. Detection sensitivity in tumor depth determination. (a) Illustration of evaluation regions and indentation depth zones. (b) Detection sensitivity of normal and shear force in determining the embedded tumor in different indentation depth zones, regarding the tumor depth. (c) Detection sensitivity of normal and shear force in determining the embedded tumor in different indentation depth zones for all tissue models.

shallow zone, the A_g value of the shear force for the shallow embedded tumor (2 mm depth) was approximately 0.75. On the other hand, the A_g values of normal force for the shallow embedded tumor and of normal and shear force for the medium (depth of 5 mm) and deep (depth of 8 mm) embedded tumors were roughly the chance level (0.5). This indicated that the shear force can only be used to distinguish between the areas with and without tumors in the shallow zone. In the medium zone, the results indicated that we can use the normal and shear forces to detect shallow and medium tumors, while deep tumors may be difficult to detect using both normal and shear forces. In the deep zone, normal or shear forces can be used to localize the tumor at different depths. Fig. 11(c) shows the sensitivity index of the force components of all tissue models in the three indentation depth zones of the sensor. Generally, the shear force revealed a better sensitivity in detecting tumors in each depression depth zone.

3) TUMOR SIZE DETERMINATION

For tumor size determination, we investigated the capability of the force components in detecting tumor edges. Eight evaluation regions were set horizontally in the tissue model (Fig. 12(a)). To detect the tumor edges, we distinguished

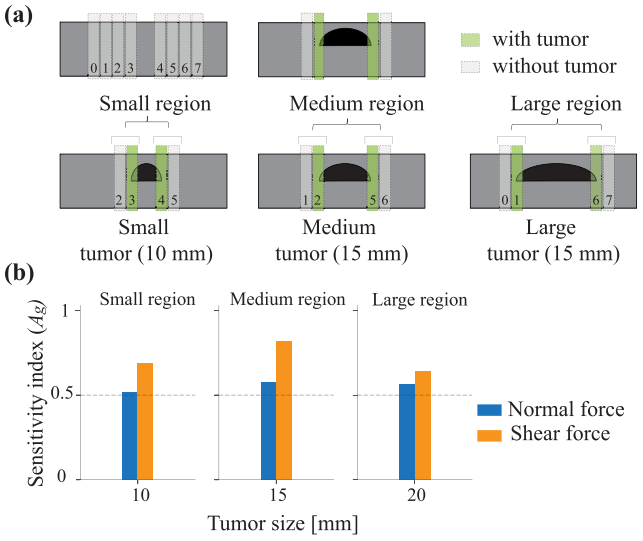

FIGURE 12. Detection sensitivity in tumor size determination. (a) Illustration of evaluation regions. (b) Detection sensitivity of normal and shear force in determining the edge of embedded tumors in the evaluation regions, regardless of the tumor depth.

tissue regions with and without tumors in the tumor edge region. In the models with small tumors (10 mm), the tumors were present in regions 3 ($X \in$ [–7 mm, –5 mm]) and 4 ($X \in$ [5 mm, 7 mm]), whereas the tumor was absent in regions 2 ($X \in$ [–9 mm, –7 mm]) and 5 ($X \in$ [7 mm, 9 mm]). Here, we defined the small region as regions 3 and 4 and regions 2 and 5. With this detection method, we observed that the edges of small tumors were located in the small region. Similarly, the medium region consists of evaluation regions 1 ($X \in$ [–11 mm, –9 mm]),6 ($X \in$ [9 mm, 11 mm]), 2, and 5. The large region consisted of the evaluation regions 0 ($X \in$ [–13 mm, –11 mm]), 7 ($X \in$ [11 mm, 13 mm]), 1, and 6. The edges of the medium (15 mm) and large (20 mm) tumors were located in the medium and large regions, respectively. The A_g value was also used to evaluate the normal and shear force sensitivities for tumor edge detection. Furthermore, the results of the tumor depth determination indicated that the contact force information was not effective in detecting several tumors of medium or deep depth in the shallow and medium depth zones. The sensitivity of the force components for tumor depth detection had the best performance in the deep indentation depth zone. Thus, we decided to evaluate their sensitivity to tumor size determination in the deep zone only.

Fig. 12(b) shows the sensitivity index of the two force components for detecting the tumor edge in the deep zone. The results indicated that the edge of small embedded tumors can be detected in the small region, the medium tumor in the medium region, and the large tumor in the large region. Generally, the shear force also exhibited better sensitivity in detecting tumor edges (or tumor size determination) compared with the normal force.

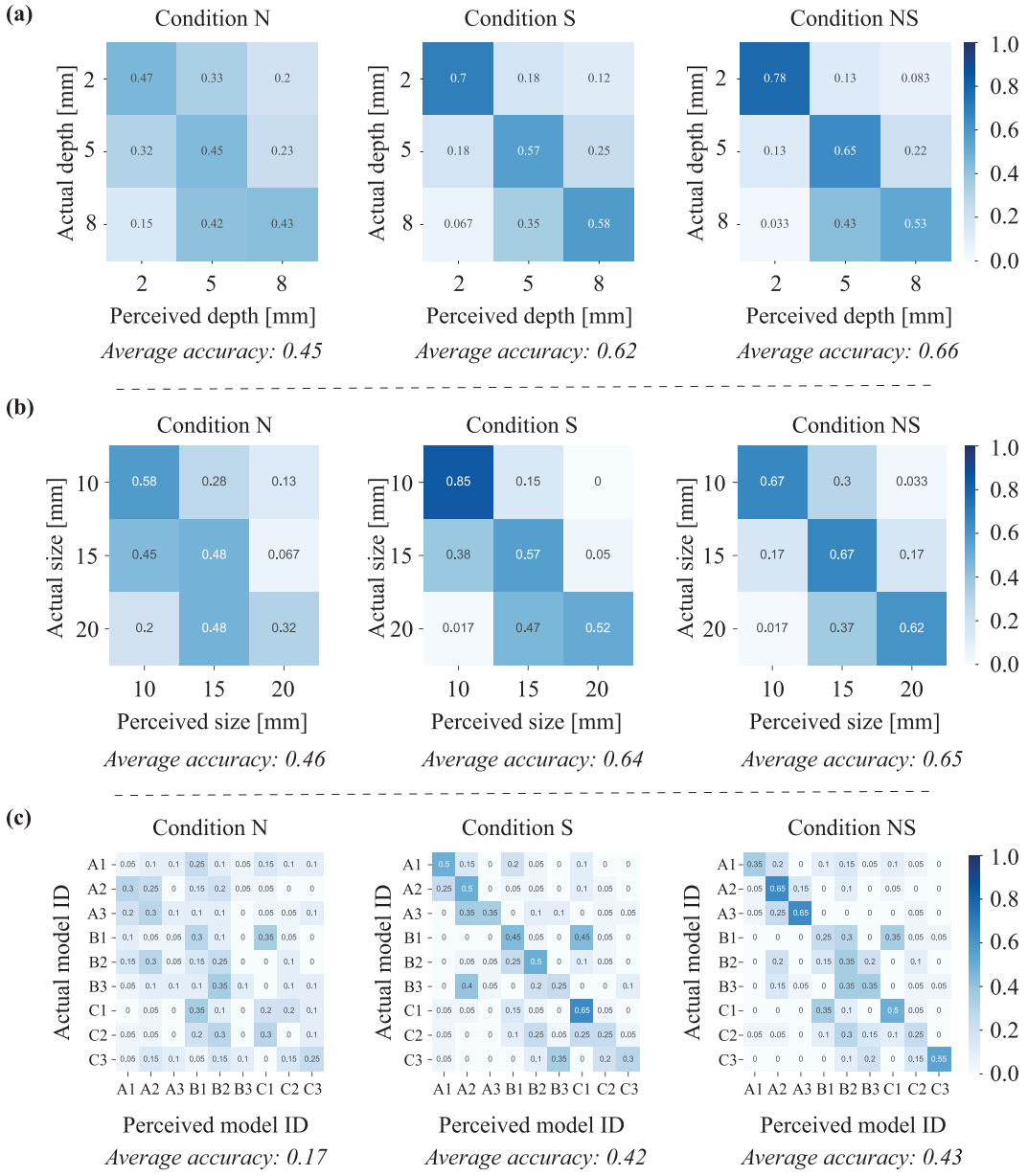

FIGURE 13. Confusion matrices of the participant's performance on tumor characterization under three feedback conditions. (a) Results of tumor depth identification. (b) Results of tumor size identification. (c) Results of both tumor depth and size identification.

B. PSYCHOPHYSICAL EXPERIMENT

Fig. 13 shows the confusion matrices of the participants' responses in the three feedback conditions provided by the tactile display for the three tumor depths and three tumor sizes of the nine tissue models. The average accuracy for each feedback condition is also listed below each confusion matrix. The results indicated that condition NS had the best matching performance, followed by conditions S and N.

Statistical tests with a significance level of 0.05 were used to investigate the effect of the feedback conditions on the participant's performance in determining the tumor depth and tumor size independently. Fig. 14(a) shows the accuracy of all participants' identification of the tumor depth and size in the three conditions. The accuracy is expressed as the ratio of correct identification responses (N_{correct}) to the number of identification targets (N_{target}) (multiplied by 100 to turn it into a percentage) using the following equation:

$$\text{Accuracy} = \frac{N_{\text{correct}}}{N_{\text{target}}}. \tag{6}$$

The accuracy data were normally distributed using the Shapiro–Wilk test. The data also passed Mauchly's test of sphericity. Thus, a repeated–measures analysis of

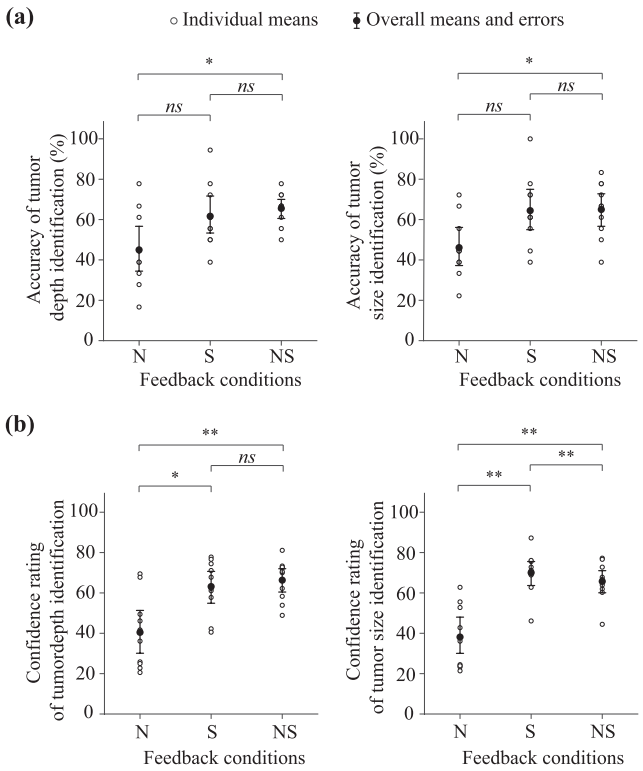

FIGURE 14. Summary of identification performance for three experimental conditions (N, S, and NS). (a) Accuracy of tumor depth and tumor size identification. (b) The confidence ratings of tumor depth and tumor size identification. ** indicates $p < 0.01$, * indicates $p < 0.05$, and *ns* indicates $p > 0.05$.

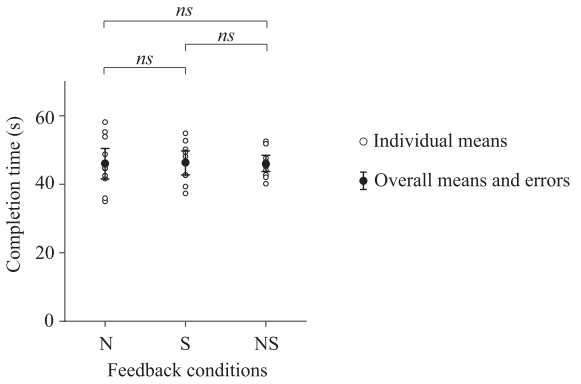

FIGURE 15. Completion time of participants in their tumor characterization. * indicates $p < 0.05$, and *ns* indicates $p > 0.05$.

variance (ANOVA) was conducted to evaluate the effect of the feedback conditions on the identification accuracy. The ANOVA test results indicated that the feedback condition significantly affected the identification accuracy of tumor depth ($p = 0.013$) and tumor size ($p = 0.03$). Multiple comparisons using paired t–tests with Bonferroni corrections indicated that a significant difference in determining tumor depth ($p = 0.012$) and tumor size ($p = 0.024$) between conditions N and NS, whereas no significant difference was observed in the identification accuracy between condition S and the other feedback conditions.

The average confidence ratings of the participants for their identification of each tumor depth and tumor size under the three feedback conditions are shown in Fig. 14(b). The rating data were normally distributed based on the Shapiro–Wilk test. Mauchly's test of sphericity revealed that the sphericity assumption was violated ($p < 0.01$). A repeated–measures ANOVA with a Greenhouse–Geisser correction indicated a statistically significant difference between the means of the three feedback conditions for both the depth ($p < 0.01$) and the size ($p < 0.01$) determination of the embedded tumors. Paired t–tests revealed that there were significant differences in confidence ratings between conditions N and NS ($p < 0.01$ for both depth and size identifications) and between conditions N and S ($p = 0.02$ for depth identification, and $p < 0.01$ for size identification). Furthermore, a statistically significant difference was observed between conditions S and NS in tumor size identification ($p < 0.01$), but there was no significant difference between the two conditions for tumor depth determination ($p = 0.23$).

We also investigated the effect of the feedback conditions on the participants' time to complete the palpation task. The completion time data (Fig. 15) passed the Shapiro–Wilk normality test and Mauchly's sphericity test. The results of the repeated-measures ANOVA indicated that the feedback conditions had no significant effect on the participants' completion time ($p = 0.96$). The average completion time of the participants in the three feedback conditions was approximately 46 s.

IV. DISCUSSION

A. FUNDAMENTAL EXPERIMENTS

The results of the fundamental experiments indicated the response of normal and shear forces during tissue palpation in nine tissue models. The tumor depth information was obtained by estimating the indentation depth of the force sensor at which the tumor was present. According to the Pearson correlation tests, the normal force indicated a high linear correlation with the indentation depth of the sensor, whereas the shear force was slightly correlated with the indentation depth over the entire tissue area that was examined. Thus, it is better to use normal force information to estimate the indentation depth of the sensor.

SDT was used to evaluate the capability of the force components to distinguish between the tissue areas with and without tumors. SDT is a better method for evaluating the results of fundamental experiments than machine learning–based methods, which tends to cause overfitting on a small dataset [10]. In manual tissue palpation, although surgeons might perceive the indentation depth of the sensor based on force feedback information, achieving the same indentation every time as in robot-assisted tissue palpation is challenging. However, surgeons may have the ability to reach the relative indentation of the sensor during palpation. Thus, in the fundamental experiment, we investigated

the capability of the contact force components to determine the tumor in three indentation depth zones, which might be achieved by manual tissue palpation. Fig. 11(b) and 11(c) show the sensitivity indices of the two force components in tumor detection for the three tumor depths in the three indentation depth zones. The shear force indicated a higher sensitivity at each indentation depth zone compared with the normal force. The small effect of normal force on tumor detection might stem from the boundary conditions of the examined tissue. In actual scenarios, human tissue is located on top of other organs or soft tissue. Thus, the human tissue might be deformed during palpation with probes or sensors, causing a decrease in the normal force response. In this study, we used a polyurethane foam plate to simulate the underlying soft tissue. Here, the shear force exhibited better sensitivity in tumor localization, as reported in [32]. Other studies achieved better tumor characterization results with the normal force because the experimental tissue were placed on rigid bases [7], [15]. According to the fundamental results, both the normal and shear forces should be used to identify the depth of the embedded tumor.

The tumor size information can be obtained by localizing the two edges of the embedded tumor. The sensitivity indices of the contact force responses in the deep zones for detecting tumor edges were evaluated. Based on the results of the fundamental experiments, we could detect the tumor edge of the small embedded tumor in the small region, the medium tumor in the medium region, and the large tumor in the large region. Generally, the shear force also exhibited higher sensitivity for tumor edge detection compared with the normal force component. Thus, the use of shear force information is considered an effective method of determining tumor size.

Fundamental experiments demonstrated the possibility of using the contact force component information (normal and shear forces) to characterize the tumor. The experimental results support the hypothesis of the proposed palpation method. Normal force information can be used to estimate the indentation depth of the sensor. The tumor depth can be obtained by localizing the tumor using shear force information at a given indentation depth. The tumor size can be determined in the deep zone by relying only on shear force information. From the results, a tactile display with normal and shear force feedback functions, such as our developed tactile display (Sup–Ring), can be a good candidate for identifying tumor characteristics.

B. PSYCHOPHYSICAL EXPERIMENTS

The psychophysical experiments indicated the effect of tactile feedback conditions produced by the SuP–Ring on the participant's performance in tumor characteristics identification. For tumor depth identification, higher determination accuracy and higher confidence were obtained in condition NS than in condition N. The results revealed that additional shear feedback was necessary to detect the tumor at a given depth. In addition, the mean accuracy of identifying the tumor depth under condition S was up to 62 %, which was slightly lower than that under condition NS. However, there was no statistically significant difference in accuracy and participant confidence under the two conditions. A possible reason for this is that the participant received kinesthetic feedback on their palms in addition to the tactile feedback in the tissue palpation tasks. Kinesthetic feedback is often associated with normal tactile feedback. This might enable the participants to estimate the indention depth of the sensor using kinesthetic feedback under condition S. However, in actual surgery, the perception of kinesthetic feedback tends to be impaired owing to the friction between the surgical tool shaft and a trocar [33]. Meanwhile, the normal tactile feedback, which represented the normal contact force at the tip of the palpated tool, was not affected by trocar friction. Thus, we consider that normal feedback is necessary to determine the tumor during actual surgery. A further study will investigate the effect of kinesthetic feedback and normal tactile feedback on the determination of tumor characteristics in actual tissue palpation.

For tumor size identification, the participants responded more accurately and confidently to tumor size when both normal and shear feedback were provided (condition NS), compared with when only normal feedback was provided (condition N). The average accuracy of tumor size identification in condition NS was 65 %. The accuracy value was slightly lower than the accuracy of participants' performance (73 %) in the task of identifying the size of 10 rectangles generated using the MRF haptic display [23]. However, the MRF display in this study was a large device (with a base of 200 mm $\times$ 200 mm), and it presented rectangles of large size (ranging from 20 mm $\times$ 20 mm to 155 mm $\times$ 155 mm). Thus, MRF displays are not suitable for surgical applications. Meanwhile, our tactile display has significant clinical advantages, such as simple structure, small size, low cost, disposability, and sterilizability [25]. In the other feedback conditions, there was no difference in the participants' performance in identifying tumor size between conditions S and NS. However, the participants responded more confidently when only the shear feedback (condition S) was represented. In condition NS, dynamic normal feedback of the SuP–Ring could have interfered with the participant's perception of shear feedback, causing them to lose confidence in identifying the tumor size [25]. Furthermore, in the determination of tumor depth under condition NS, the dynamic effect between the two feedback components may have caused the participant to lose confidence in determining the tumor location. However, providing normal feedback might have caused them to be more confident in estimating the indentation depth of the sensor. Thus, there was no significant difference between conditions S and NS in participants' confidence in identifying the tumor depth. In the future, we plan to investigate the dynamic effects between the two tactile feedback components of tactile displays.

The participants' completion time was not significantly affected by the tactile feedback conditions in the palpation tasks. These results indicate that participants may need a certain period, called the standard period, to determine the tumor features. In this experiment, the average completion time was approximately 46 s, which was considered a standard period. In some conditions, participants could rapidly identify the tumor features but needed the standard time to confirm this information. However, in other feedback conditions, if the tactile feedback did not provide much useful information, the participant could assume that increasing the time spent on tissue palpation would not provide any further useful information. Therefore, the standard time may be sufficient for the participants to complete the tissue palpation task, regardless of feedback conditions.

C. LIMITATIONS AND FUTURE WORKS

Generally, the experiments indicated that the users had a high potential in identifying the depth and size of embedded tumors when they were provided with both normal and shear feedback using a tactile display. However, some problems should be addressed to enhance tissue characterization performance.

First, we consider the issues of using the SuP–Ring in actual tissue palpation scenarios. In actual surgery, tumors often have complex structures, and the contact force when palpating actual tissue often consists of three-dimension (3D) force components, including 1D normal force component (along the z–axis) and 2D shear force component (along the x–axis and y–axis). Simply moving the palpated tool in a single path, as in the palpation task performed in the study, is not sufficient to grasp the characteristics of the tumor. Moreover, because the SuP–Ring has two degrees of freedom (2–DoF), the tactile display could not represent the three components of the contact force. However, the tumor can still be assessed using the SuP–Ring by moving the palpated tool in parallel paths to scan the entire tissue surface. This technique is known as the vertical strip technique, a common global palpation technique for soft tissue examinations [34]. In addition, the superposition of the two shear force components could be used as an input for the tactile display's shear feedback to determine the tumor features. By using the above methods, the SuP–Ring can maintain its advantage in terms of simplicity. An alternative approach is to modify the structure of the SuP–Ring to represent 3–DoF tactile feedback. The effect of the 3–DoF tactile display will be investigated in a future study. Furthermore, although our developed tactile display has significant clinical advantages, it does not provide high–resolution tactile feedback [25]. This may cause a reduction in the user's ability to determine tumor features. We plan to improve the resolution of the tactile feedback in further studies to obtain a better determination performance.

Second, in the tissue palpation task, the participants conducted the training experiments and practiced again before conducting the practical task. However, the training time might have been insufficient for them to remember the feedback perception properly and provide consistent estimations. If the participants were trained for a longer time, they would determine the tumor characteristics more accurately.

Finally, all participants in this study were novices, which enabled us to fairly evaluate the effectiveness of tactile feedback for tissue characterization. In future research, we plan to perform experiments with skilled surgeons. We consider that experts will perform better in tumor characterization because they have higher surgical skills and more experience in tissue palpation. The effect of participants' skills and experience will be investigated in future studies.

V. CONCLUSION

In this study, we investigated the capability of tactile feedback in characterizing tumors during laparoscopic tissue palpation. We proposed a palpation strategy to identify tumor features, such as depth and size. Contact force components (normal and shear force) were used to determine the indentation depth of the palpated sensor and to detect the tumor area and the edges of the tumor. The tumor depth was determined by detecting the presence of the tumor at a given indentation depth of the sensor. The size of the tumor can be derived by localizing the tumor edges. The responses of the contact force components when palpating the tissue were indicated through fundamental experiments with nine artificial phantom tissue models. The experimental results indicated that both normal and shear force information should be used to determine tumor depth. Additionally, the shear force provides a higher sensitivity for determining tumor size. Twelve participants without a medical background performed tissue palpation tasks to identify the depth and size of the embedded tumor within the tissue model. The normal and shear force feedback during tissue palpation was provided to the participants using our developed pneumatic tactile display. The tactile display has high clinical applicability owing to its simple structure, light weight, and sterilizability. In the experiment, we evaluated the effectiveness of tactile feedback on the participants' identification performance. The experimental results indicated that the participants identified the tumor characteristics more correctly when provided with both normal and shear feedback. However, the tactile display requires further improvements to enhance the user's identification performance.

REFERENCES

[1] W. Semere, M. Kitagawa, and A. M. Okamura, "Teleoperation with sensor/actuator asymmetry: Task performance with partial force feedback," in *Proc. HAPTICS,* Chicago, IL, USA, 2004, pp. 121–127.

[2] C. R. Wagner, N. Stylopoulos, and R. D. Howe, "The role of force feedback in surgery: Analysis of blunt dissection," in *Proc. 10th Symp. Haptic Interface Virtual Environ. Teleoperator Syst.*, Orlando, FL, USA, 2002, pp. 68–74.

[3] K. Sasaki, M. Matsuda, Y. Ohkura, Y. Kawamura, M. Hashimoto, K. Ikeda, H. Kumada, and G. Watanabe, "Minimum resection margin should be based on tumor size in hepatectomy for hepatocellular carcinoma in hepatoviral infection patients: Base resection margin on tumor size," *Hepatol. Res.*, vol. 43, no. 12, pp. 1295–1303, Feb. 2013.

[4] B. Liu, T. Liu, M. Su, Y.-Q. Ma, B.-F. Zhang, Y.-F. Wang, B.-Y. Hu, and Y.-L. Chen, "Improving the surgical effect for primary liver cancer with intraoperative fluorescence navigation compared with intraoperative ultrasound," *Med. Sci. Monitor*, vol. 25, pp. 3406–3416, May 2019.
[5] M. Li, H. Liu, A. Jiang, L. D. Seneviratne, P. Dasgupta, K. Althoefer, and H. Wurdemann, "Intra-operative tumour localisation in robot-assisted minimally invasive surgery: A review," *Proc. Inst. Mech. Eng. H, J. Eng. Med.*, vol. 228, no. 5, pp. 509–522, May 2014.
[6] I. B. Wanninayake, P. Dasgupta, L. D. Seneviratne, and K. Althoefer, "Air-float palpation probe for tissue abnormality identification during minimally invasive surgery," *IEEE Trans. Biomed. Eng.*, vol. 60, no. 10, pp. 2735–2744, Oct. 2013.
[7] M. Sadeghi-Goughari, A. Mojra, and S. Sadeghi, "Parameter estimation of brain tumors using intraoperative thermal imaging based on artificial tactile sensing in conjunction with artificial neural network," *J. Phys. D, Appl. Phys.*, vol. 49, no. 7, Jan. 2016, Art. no. 075404.
[8] S. Lederman and R. Klatzky, "Sensing and displaying spatially distributed fingertip forces in haptic interfaces for teleoperator and virtual environment systems," *Presence*, vol. 8, no. 1, pp. 86–103, Feb. 1999.
[9] K. Hoyt, B. Castaneda, M. Zhang, and P. Nigwekar, "Tissue elasticity properties as biomarkers for prostate cancer," *Cancer Biomarkers*, vol. 4, nos. 4–5, pp. 213–225, 2008.
[10] J. C. Gwilliam, Z. Pezzementi, E. Jantho, A. M. Okamura, and S. Hsiao, "Human vs. Robotic tactile sensing: Detecting lumps in soft tissue," in *Proc. IEEE Haptics Symp.*, Waltham, MA, USA, Mar. 2010, pp. 21–28.
[11] A. Talasaz and R. V. Patel, "Telerobotic palpation for tumor localization with depth estimation," in *Proc. IEEE/RSJ Int. Conf. Intell. Robots Syst.*, Tokyo, Japan, Nov. 2013, pp. 463–468.
[12] T. Yamamoto, B. Vagvolgyi, K. Balaji, L. L. Whitcomb, and A. M. Okamura, "Tissue property estimation and graphical display for teleoperated robot-assisted surgery," in *Proc. IEEE Int. Conf. Robot. Autom.*, Kobe, Japan, May 2009, pp. 4239–4245.
[13] H. Liu, D. P. Noonan, B. J. Challacombe, P. Dasgupta, L. D. Seneviratne, and K. Althoefer, "Rolling mechanical imaging for tissue abnormality localization during minimally invasive surgery," *IEEE Trans. Biomed. Eng.*, vol. 57, no. 2, pp. 404–414, Feb. 2010.
[14] P. Richard and P. Coiffet, "Human perceptual issues in virtual environments: Sensory substitution and information redundancy," in *Proc. 4th IEEE Int. Workshop Robot. Hum. Commun.*, Tokyo, Japan, Jun. 1995, pp. 301–306.
[15] S. M. Hosseini, M. Amiri, S. Najarian, and J. Dargahi, "Application of artificial neural networks for the estimation of tumour characteristics in biological tissues," *Int. J. Med. Robot. Comput. Assist. Surg.*, vol. 3, no. 3, pp. 235–244, Sep. 2007.
[16] B. Xiao, W. Xu, J. Guo, H.-K. Lam, G. Jia, W. Hong, and H. Ren, "Depth estimation of hard inclusions in soft tissue by autonomous robotic palpation using deep recurrent neural network," *IEEE Trans. Autom. Sci. Eng.*, vol. 17, no. 4, pp. 1791–1799, Oct. 2020.
[17] J. Palacio-Torralba, R. L. Reuben, and Y. Chen, "A novel palpation–based method for tumor nodule quantification in soft tissue—Computational framework and experimental validation," *Med. Biol. Eng. Comput.*, vol. 58, no. 6, pp. 1369–1381, Apr. 2020.
[18] F. Saleheen and C.-H. Won, "Dynamic positioning sensing system for estimating size and depth of embedded object," in *Proc. IEEE SENSORS*, Busan, South Korea, Nov. 2015, pp. 1–4.
[19] R. D. Howe, W. J. Peine, D. A. Kantarinis, and J. S. Son, "Remote palpation technology," *IEEE Eng. Med. Biol. Mag.*, vol. 14, no. 3, pp. 318–323, May 1995.
[20] R. L. Feller, C. K. L. Lau, C. R. Wagner, D. P. Perrin, and R. D. Howe, "The effect of force feedback on remote palpation," in *Proc. Int. Conf. Robot. Autom.*, New Orleans, LA, USA, 2004, pp. 782–788.
[21] L. Min, L. Shan, T. Nanayakkara, L. D. Seneviratne, P. Dasgupta, and K. Althoefer, "Multi-fingered haptic palpation using pneumatic feedback actuators," *Sens. Actuators A, Phys.*, vol. 218, no. 10, pp. 132–141, Oct. 2014.
[22] M. Bianchi, J. C. Gwilliam, A. Degirmenci, and A. M. Okamura, "Characterization of an air jet haptic lump display," in *Proc. EMBC*, Boston, MA, USA, 2011, pp. 3467–3470.
[23] R. Rizzo, A. Musolino, and L. A. Jones, "Shape localization and recognition using a magnetorheological-fluid haptic display," *IEEE Trans. Haptics*, vol. 11, no. 2, pp. 317–321, Apr. 2018.
[24] T. Fukuda, Y. Tanaka, A. M. L. Kappers, M. Fujiwara, and A. Sano, "A pneumatic tactile ring for instantaneous sensory feedback in laparoscopic tumor localization," *IEEE Trans. Haptics*, vol. 11, no. 4, pp. 485–497, Oct. 2018.
[25] H. H. Ly, Y. Tanaka, and M. Fujiwara, "SuP-ring: A pneumatic tactile display with substitutional representation of contact force components using normal indentation," *Int. J. Med. Robot. Comput. Assist. Surg.*, vol. 17, no. 6, Dec. 2021.
[26] J. Konstantinova, G. Cotugno, P. Dasgupta, K. Althoefer, and T. Nanayakkara, "Palpation force modulation strategies to identify hard regions in soft tissue organs," *PLoS ONE*, vol. 12, no. 2, Feb. 2017, Art. no. e0171706.
[27] C. F. Guimarães, L. Gasperini, A. P. Marques, and R. L. Reis, "The stiffness of living tissues and its implications for tissue engineering," *Nature Rev. Mater.*, vol. 5, no. 5, pp. 351–370, Feb. 2020.
[28] R. Masuzaki, R. Tateishi, H. Yoshida, T. Sato, T. Ohki, T. Goto, H. Yoshida, S. Sato, Y. Sugioka, H. Ikeda, S. Shiina, T. Kawabe, and M. Omata, "Assessing liver tumor stiffness by transient elastography," *Hepatol. Int.*, vol. 1, no. 3, pp. 394–397, Jul. 2007.
[29] J. Han, M. Kamber, and J. Pei, "Data transformation and data discretization," in *Data Mining: Concepts Techniques*. Oxford, U.K.: Morgan Kaufmann, 2012, pp. 111–118.
[30] N. A. Macmillan and C. D. Creelman, *Detection Theory: A User's Guide*. Philadelphia, PA, USA: Psychology Press, 2005.
[31] S. Coren, *The Left–Hander Syndrome: The Causes and Consequences of Left–Handedness*.New York, NY, USA: McGraw-Hill, 2000, pp. 37–38.
[32] H. H. Ly, Y. Tanaka, and M. Fujiwara, "A tactile sensor using the acoustic reflection principle for assessing the contact force component in laparoscopic tumor localization," *Int. J. Comput. Assist. Radiol. Surg.*, vol. 16, no. 2, pp. 289–299, Jan. 2021.
[33] E. Westebring-Van-Der-Putten, R. Goossens, J. J. Jakimowicz, and J. Dankelman, "Haptics in minimally invasive surgery—A review," *Minimally Invasive Therapy*, vol. 17, no. 1, pp. 3–16, 2008.
[34] N. Wang, G. J. Gerling, R. M. Childress, and M. L. Martin, "Quantifying palpation techniques in relation to performance in a clinical prostate exam," *IEEE Trans. Inf. Technol. Biomed.*, vol. 14, no. 4, pp. 1088–1097, Jul. 2010.

HOANG HIEP LY received the B.E. degree (Hons.) in mechatronics from the Hanoi University of Science and Technology, Vietnam, in 2015, and the M.E. degree in mechanical engineering from the Nagoya Institute of Technology, Japan, in 2018, where he is currently pursuing the Ph.D. degree. Since 2019, he has been a Research Fellow with the Japan Society for the Promotion of Science (DC1). His research interests include the development of haptic devices, medical devices, and robotic applications. His awards and honors include the 21st Annual Conference of International Society for Computer Aided Surgery ISCAS–CARS Best Poster Award, in 2017, and the Miura Award from the Japan Society of Mechanical Engineers (JSME), in 2018.

YOSHIHIRO TANAKA (Member, IEEE) skipped from undergraduate school to graduate school and received the M.S. and Ph.D. degrees from Tohoku University, Japan, in 2003 and 2006, respectively. He was a Research Fellow with the Japan Society for the Promotion of Science, in 2005. In 2006, he was a Research Associate with the Nagoya Institute of Technology, Japan. He was a Visiting Researcher with Utrecht University, The Netherlands, in 2011; a Visiting Associate Professor with Fujita Health University, Japan, from 2015 to 2019; a PRESTO Researcher of the Japan Science and Technology Agency, from 2014 to 2018; and an Associate Professor with the Nagoya Institute of Technology, from 2015 to 2021, where he has been a Professor with the Graduate School of Engineering, since 2021. His research interests include haptic perception, tactile interfaces, tactile device design, and human–human/robot cooperation with shared haptic perception. He is a member of the Society of Instrument and Control Engineers (SICE), the Robotics Society of Japan (RSJ), the Virtual Reality Society of Japan (VRSJ), and the Japan Society of Mechanical Engineers (JSME). He was a recipient of the Robotics Society of Japan Young Investigation Excellence Award, in 2010, and the Japan Society of Mechanical Engineers Young Engineer Awards, in 2011. He has also been an Associate Editor of *Advanced Robotics*, since 2019, and the IEEE TRANSACTIONS ON HAPTICS, since 2020.

MICHITAKA FUJIWARA received the graduate and Ph.D. degrees from the School of Medicine, Nagoya University, in 1987 and 2003, respectively. From 1987 to 1993, he was a resident of the Ichinomiya Municipal Hospital and he did surgical training and research at the Department of Surgery II, Nagoya University, from 1993 to 2003. He worked with Nagoya University under various positions, which includes an Associate Professor with the Department of Endoscopic Surgery, from 2004 to 2011; an Associate Professor with the Postgraduate School of Medicine, from 2011 to 2013; and an Associate Professor with the Clinical Simulation Center, Postgraduate School of Medicine, from 2013 to 2020. Since 2020, he has been a Professor with the Department of Medical Equipment and Supplies Management, Nagoya University Hospital, and the Medical xR Center, Nagoya University Graduate School of Medicine. His major research interests include navigation surgery using new imaging technology and surgical education using virtual reality simulator. He is a member of the International Gastric Cancer Association, the International Society of Surgery (ISS), Society of American Gastrointestinal and Endoscopic Surgeons (SAGES), and the International Association of Surgeons, Gastroenterologists and Oncologists (IASGO). He also serves as an Editorial Board Member for Gastric Cancer. He received the Young Researcher's Award of the Japanese Gastric Cancer Association, in 1998, and the 17th World Congress of International Society for Digestive Surgery Best Poster Award, in 2000.